doi:10.1038/nature11670

Supplementary note 1 | Evidence for a general requirement of the head module.
To investigate whether the head module generally functions in Pol II transcription, particularly also at constitutive housekeeping promoters, we performed *in vitro* transcription assays on three different Pol II promoter templates: the TATA-containing *Sc HIS4* promoter, the TATA-less *Sc TMT1* promoter[1] and the constitutive housekeeping *Sc ACT1* promoter (see Methods). All three promoters supported Pol II transcription in a yeast nuclear extract (Fig. 2b). In contrast, an extract from the temperature-sensitive strain *srb4-138* (ref. 2) (also called *srb4*^{ts} (ref. 3)) was inactive, but addition of recombinant head module enabled transcription (Fig. 2b). These results agree with a general function of the head module at all Pol II promoters[3].

Supplementary note 2 | An alternative position of Med8C–Med18 in *Sp* head module crystals.
Density corresponding to the Med8C–Med18 subcomplex is weaker compared to the rest of the head module. Although this does not compromise our structure, because a refined atomic model of the Med8C–Med18 complex is available and was used in modelling, this indicates flexibility of the moveable jaw that can also be seen from higher B-factors. In addition, very weak density suggests that a minor fraction of Med8C–Med18 can adopt an alternative position in head module crystals. Due to very low occupancy and limits in resolution, this second position was excluded from refinement. The second position may be stabilized by a crystal contact between two adjacent *Sp* Med18 subunits that form a dimer similar to what was observed in *Sp* Med8C–Med18 crystals[4]. The minor second position of Med18 does not influence any of our conclusions, it however confirms the high degree of flexibility of the moveable jaw.

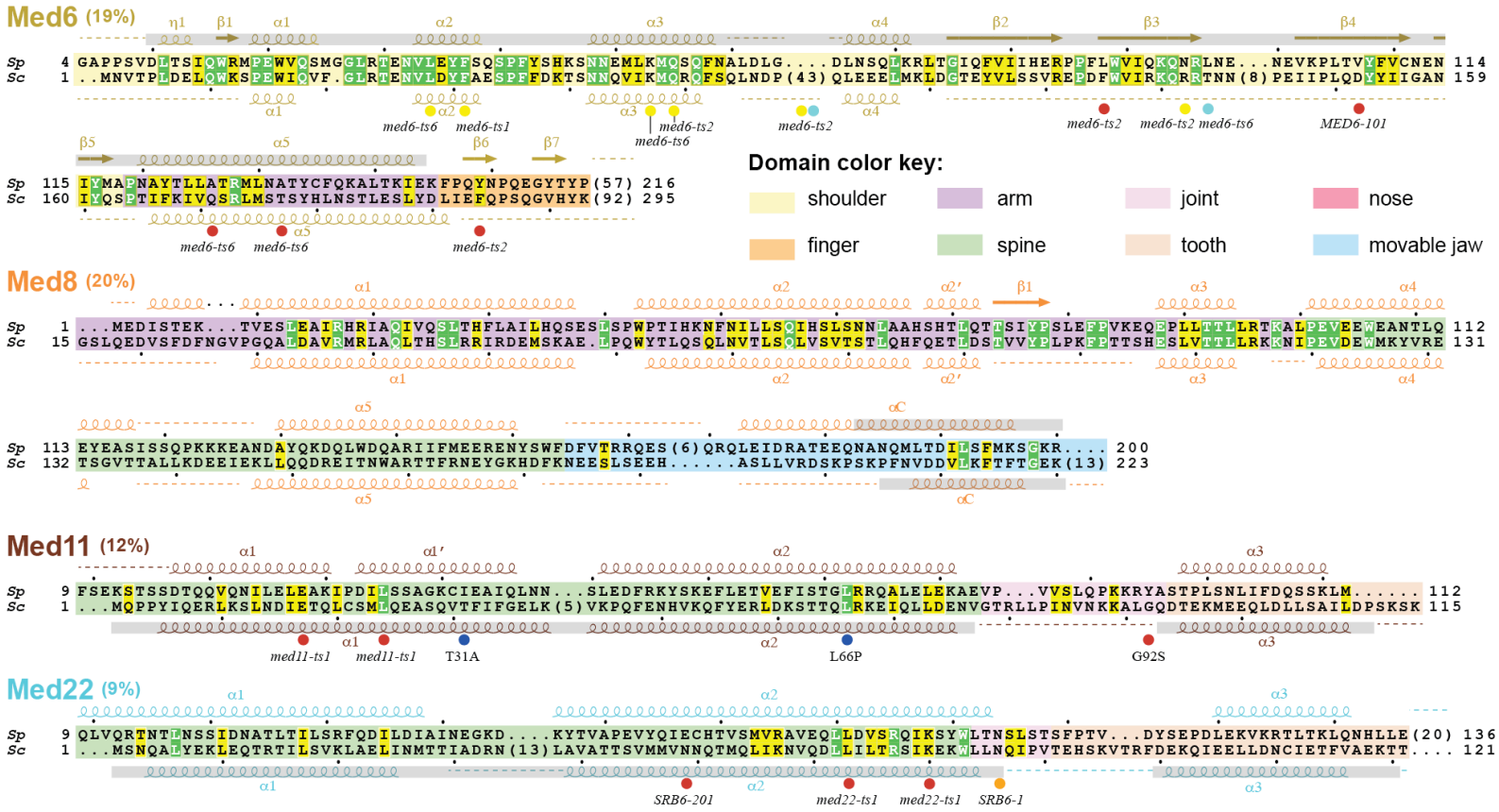
Med6 (19%)
Med8 (20%)
Med11 (12%)
Med22 (9%)
Domain color key:
shoulder
arm
joint
nose
finger
spine
tooth
movable jaw
med6-ts6
med6-ts1
med6-ts2
MED6-101
med11-ts1
T31A
L66P
G92S
SRB6-201
med22-ts1
SRB6-1

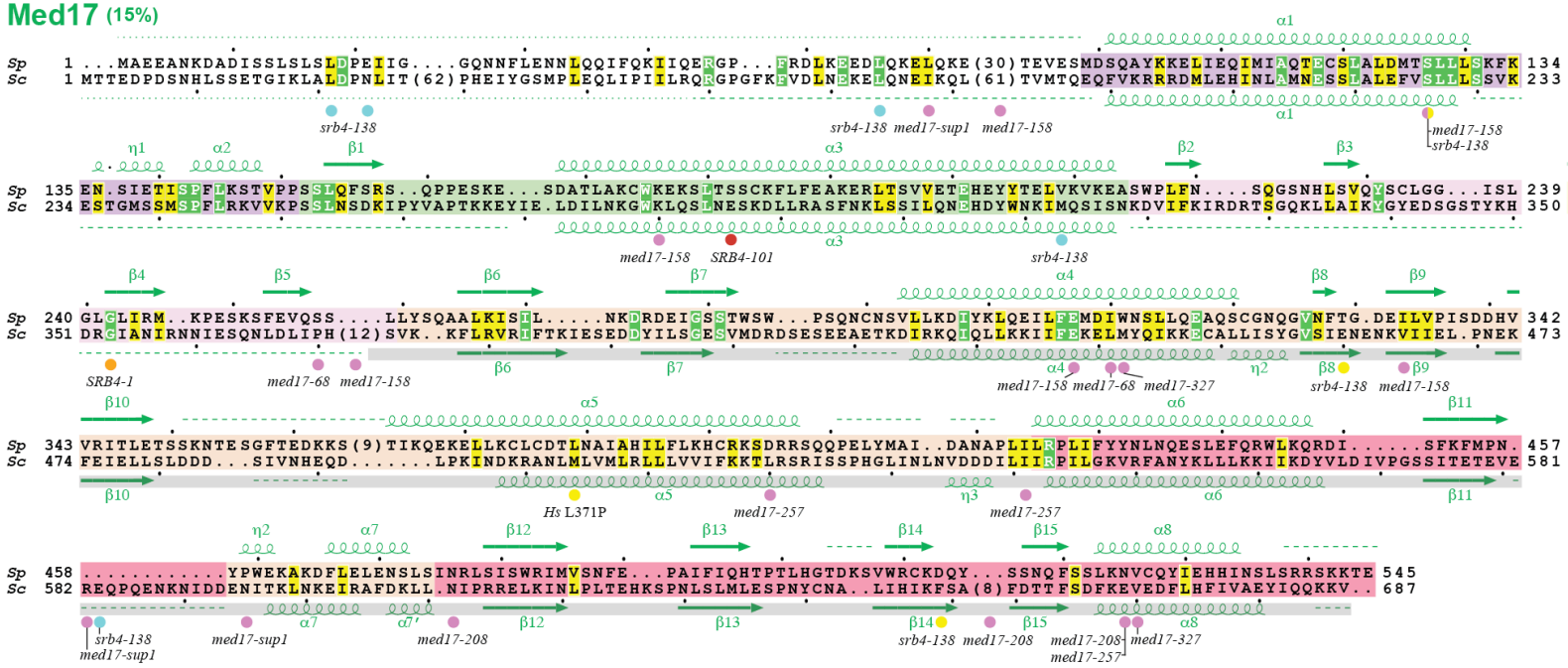
Med17 (15%)
Sp 1 ...MAEEANKDADISSLSLSLDPEIIG....GQNNFLENNLQQIFQKIIQERGP...FRDLKPEDLQKELQKE(30)TEVESMDSQAYKKELIEQIMIAQTECSIPALDMTSLILLSKFK 134
Sc 1 MTTEDPDSNHLSSETGIKLALDPNLIT(62)PHEIYGSMPLEQLIPIILRQRGPGFKFVDLNEKELQNEIKQL(61)TVMTQEQFVKRRRDMLEHINLAMNESSIPALEFVSLILSSVK 233
Sp 135 EN.SIETISPFLKSTVPPSSLQFSRS..QPPESKE...SDATLAKCWKEKSLTSSCKFLFEAKERLTSVVETEHEYYTELVKVKEASWPLFN....SQGSNHLSVQYSCLGG...ISL 239
Sc 234 ESTGMSSMSPFLRKVVKPSSLNSDKIPYVAPTKKEYIE.LDILNKGWKLQSLNESKDLLRASFNKLSSILQNEHDYWNKIMQSISNKDVIFKIRDRTSGQKLLAIKYGYEDSGSTYKH 350
Sp 240 GLGLIRM..KPESKSFEVQSS....LLYSQAALKISTL.....NKDRDEIGSSTWSW...PSQNCNSVLLKDIYKLQEILFEMDIWNSLLQEAQSCGNQGVNFTG.DEILVPISDDHV 342
Sc 351 DRGIANIRNNIESQNLDLIPH(12)SVK..KFLRVRTFTKIESEDDYILSGESVMDRDSESEEAETKDIRKQIQLLKKIIFEKELMYQIKKECALLISYGVSIENENKVIIEL.PNEK 473
Sp 343 VRITLETSSKNTESGFTEDKKS(9)TIKQEKELLKCLCDTLNAIAHILFLKHCRKSDRRSQQPELYMAI..DANAPLILRPLIFYYNLNQESLEFQRWLKQRDI.....SFKFMPN. 457
Sc 474 FEIELLSLDDD...SIVNHEQD.....LPKINDKRANLMLVMLRLLLVVIFKKTLRSRISSPHGLINLNVDDDILIIRPILGKVRFANYKLLLKKIIKDYVLDIVPGSSITETEVE 581
Sp 458 .............YPWEKAKDFLELENSLSINRLSISWRIMVSNFE...PAIFIQHTPTLHGTDKSVWRCKDQY...SSNQFSSLKNVCQYIEHHINSLSRRSKKTE 545
Sc 582 REQPQENKNIDDENITKLNKEIRAFDKLL..NIPRRELKINLPLTEHKSPNLSLMLESPNYCNA..LIHIKFSA(8)FDTTFSDFKEVEDFLHFIVAEYIQQKKV.. 687
srb4-138
srb4-138 med17-sup1 med17-158
med17-158 srb4-138
med17-158 SRB4-101
srb4-138
SRB4-1
med17-68 med17-158
med17-158 med17-68 med17-327
srb4-138 med17-158
Hs L371P
med17-257
med17-257
srb4-138 med17-sup1
med17-sup1
med17-208
srb4-138 med17-208
med17-208 med17-257
med17-327

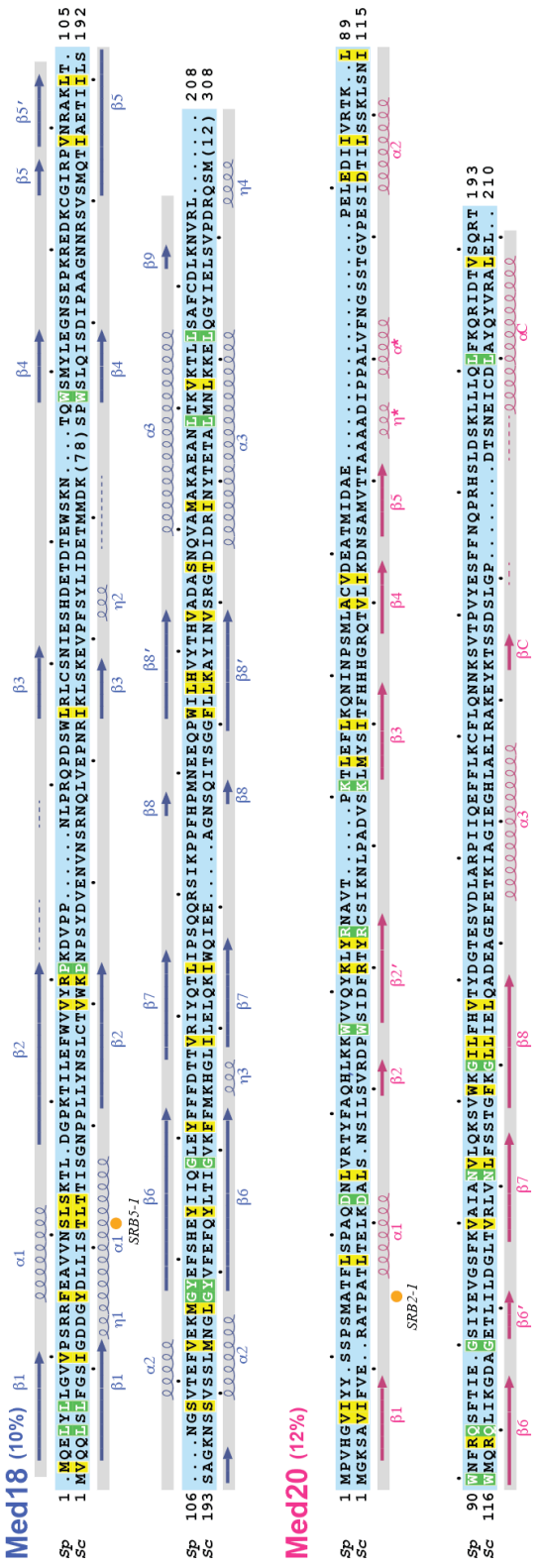
Med18 (10%)
Med20 (12%)
SRB5-1
SRB2-1

Supplementary Figure 1 | Conserved primary and secondary structure of head module subunits. Amino acid sequence alignments for Mediator head subunits Med6, Med8, Med11, Med22, Med17, Med18, and Med20 from *Schizosaccharomyces pombe* (*Sp*, top), and *Saccharomyces cerevisiae* (*Sc,* bottom). Sequence identity between *Sp* and *Sc* subunits is indicated in brackets next to the protein name. Secondary structure elements are indicated above and below the sequences as observed in the *Sp* head module structure and the *Sc* backbone model, respectively (spirals, α-helices and 3_{10}/η-helices; arrows, β-strands; dashed lines, disordered regions; dots, not present in protein variant). Regions for which high-resolution structures are available are highlighted in grey over the secondary structure elements. Residues that are invariant or conserved among the yeasts *Sp, Sc*, *Candida glabrata*, *Candida albicans*, *Ashbya gossypii*, *Kluyveromyces lactis*, and *Debaryomyces hansenii* are highlighted in green or yellow, respectively. Subunit names are given in a colour code that is used throughout (Med6, yellow; Med8, orange; Med11, brown; Med22, cyan; Med17, green; Med18, blue; Med20, magenta). Portions of the sequences forming the eight structural elements of the head module are highlighted in eight different colours (element colour key in Fig. 3). Spheres indicate known mutation sites (*med6-ts1* (ref. 5), *med6-ts2* (ref. 5), *med6-ts6* (ref. 5), *MED6-101* (ref. 6), *med11-ts1* (ref. 7), G92S[8], *srb4-138* (ref. 2,9), *SRB4-101* (ref. 5), *med17-68* (ref. 10), *med17-158* (ref. 10), *med17-208* (ref. 10), *med17-257* (ref. 10), *med17-327* (ref. 10), *med22-ts1* (ref. 7)*, Hs* L371P[11], T31A[8], L66P[8], *SRB4-1* (ref. 12), *med17-sup1* (ref. 10), *SRB5-1* (ref. 12), *SRB2-1* (ref. 13), *SRB6-1* (ref. 12), *SRB6-201* (ref. 6)) and are coloured according to their predicted effect (intrasubunit stability, yellow; intersubunit stability, red; unknown effect, cyan; suppressor of CTD truncation, orange; mutations affecting TFIIH interaction, dark blue; mutations affecting Pol II core interaction, magenta).

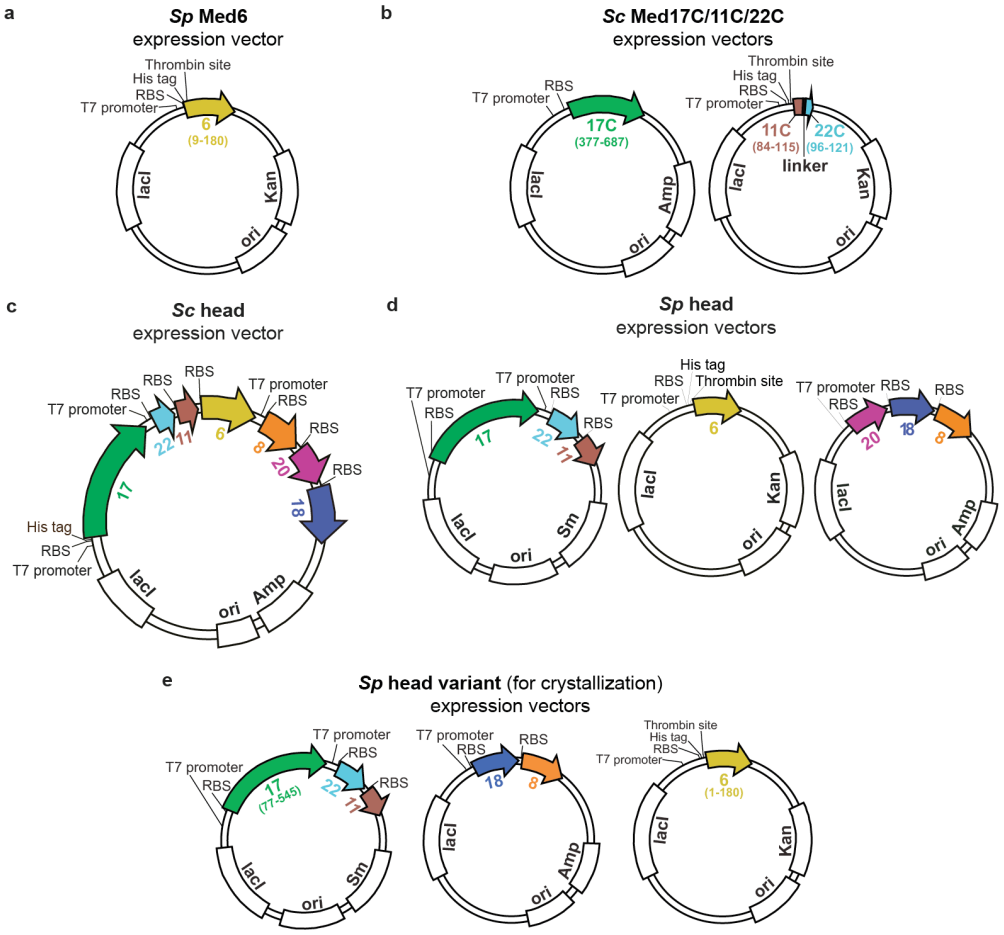

Supplementary Figure 2 | Bacterial expression vectors. Schematic representation of the plasmids used in this study for the expression of the **a,** crystallization construct of *Sp* Med6. The variant lacks only the non-essential terminal tails. **b,** *Sc* Med17C–Med11C–Med22C subcomplex. Two plasmids were used for co-expression, one expressing Med17C, the other expressing a Med11C–Med22C fusion polypeptide (see Methods). **c,** full length *Sc* head module. Co-expression was driven from a single plasmid with three T7 promoters, one for Med17 expression, one for tricistronic expression of Med22, Med11, and Med6, and one for tricistronic expression of Med8, Med18, and Med20. **d,** full length *Sp* head module. Three plasmids were used for co-expression, each harbouring a single T7 promoter, one expressing Med6, one expressing Med8, Med18, and Med20, and one expressing Med17, Med22, and Med11. **e,** *Sp* head variant used for crystallization. RBS, ribosome binding site; His tag, 6xHistidine tag; *ori*, origin of replication; *lacI*, gene encoding Lac repressor. *Sm*, *Amp* and *Kan* refer to streptomycin, ampicillin and kanamycin resistance genes, respectively.

Table 1 | Data collection and refinement statistics for Med6 and Med17C–Med11C–Med22C crystals

	Med6 (native)	Med6 (SeMet)	Med17C–Med11C–Med22C (SeMet)
Data collection			
Space group	$P2_13$	$P2_13$	R32
Cell dimensions			
a, *b*, *c* (Å)	126.0, 126.0, 126.0	125.0, 125.0, 125.0	261.2, 261.2, 47.7
Wavelength (Å)	0.91890	0.97960	0.97972
Resolution (Å)†	2.7 (2.77-2.70)*	3.4 (3.49-3.40)	3.0 (3.08-3.00)
$CC_{1/2}$‡	100.0 (32.4)	–	99.9 (17.1)
Completeness (%)	100.0 (100.0)	100.0 (100.0)	99.9 (100.0)
Redundancy	20.0 (19.3)	10.4 (10.4)	5.1 (5.2)
R_{merge} (%)	5.2 (1010.2)	16.6 (145.1)	6.1 (692.2)
$I/\sigma I$	41.4 (0.6)	11.8 (2.4)	16.5 (0.6)
Refinement			
Resolution (Å)	89–2.7		65–3.0
No. reflections	18562		12487
R_{work}/R_{free}	18.1/21.7		20.4/22.8
No. atoms			
Protein	2254		2556
Ligand			12
B-factors			
Protein	136		144
Ligand			182
R.m.s deviations			
Bond lengths (Å)	0.006		0.007
Bond angles (°)	0.967		1.218

*Highest resolution shell is shown in parenthesis.

†Resolution limits are provided using the $CC_{1/2} > 10\%$ criterion[14]. Using the traditional criterion of $I/\sigma I > 2.0$, resolution limits are 2.9 Å and 3.2 Å for Med6 and Med17C–Med11C–Med22C crystals, respectively.

‡$CC_{1/2}$ = percentage of correlation between intensities from random half-datasets[14].

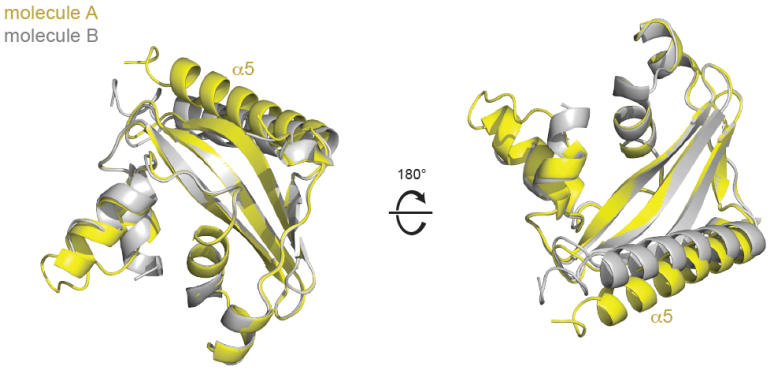

Supplementary Figure 3 | *Sp* Med6 crystal structure reveals a flexible C-terminal helix. The two molecules constituting the asymmetric unit of *Sp* Med6 crystals are superimposed and shown as yellow and grey ribbon, respectively. They differ in the orientation of their C-terminal helix α5.

Table 2 | Data collection and refinement statistics for *Sp* head module crystals

	Native	Ta_6Br_{14}	Yb-DTPA-BMA	SeMet
Data collection				
Space group	$P3_221$	$P3_221$	$P3_221$	$P3_221$
Cell dimensions				
a, *b*, *c* (Å)	145.6, 145.6, 241.6	145.4, 145.4, 233.2	146.0, 146.0, 232.6	146.0, 146.0, 238.6
Wavelength (Å)	0.99977	1.25537	1.38633	0.97940
Resolution (Å)†	3.4 (3.49-3.40)*	4.7 (4.82-4.70)	4.0 (4.1-4.0)	3.8 (3.9-3.8)
$CC_{1/2}$‡	99.9 (24.0)	99.9 (13.8)	99.7 (23.0)	99.6 (22.1)
Completeness (%)	100.0 (99.9)	99.9 (99.9)	99.7 (97.2)	99.9 (99.2)
Redundancy	10.0 (9.2)	4.6 (4.7)	5.2 (5.2)	5.2 (4.7)
R_{merge} (%)	12.5 (412.4)	9.1 (474.1)	20.4 (860.3)	18.1 (246.5)
$I/\sigma I$	15.2 (0.6)	8.4 (0.4)	7.6 (0.3)	8.9 (0.6)
Refinement				
Resolution (Å)	126–3.4			
No. reflections	41,454			
R_{work}/R_{free}	23.2/25.8			
No. atoms				
Protein	9254			
Ligand				
B-factors				
Protein	166			
Ligand				
R.m.s deviations				
Bond lengths (Å)	0.009			
Bond angles (°)	1.13			

*Highest resolution shell is shown in parenthesis.

†Resolution limits are provided using the $CC_{1/2} > 10\%$ criterion[14]. Using the traditional criterion of $I/\sigma I > 2.0$, the resolution limit of the native crystal is 3.7 Å.

‡$CC_{1/2}$ = percentage of correlation between intensities from random half-datasets[14].

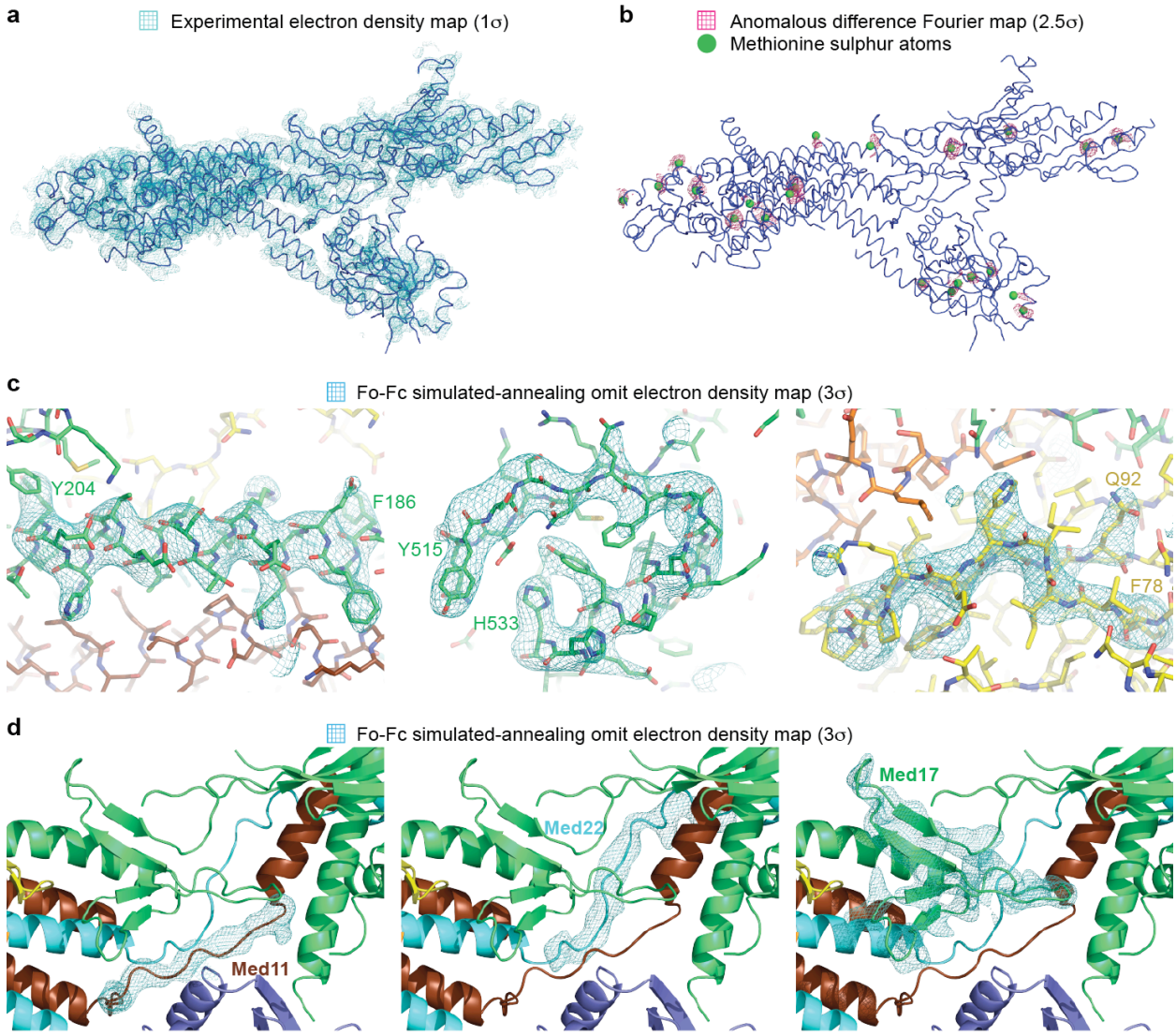

Supplementary Figure 4 | Electron density maps for the *Sp* Mediator head module. a, Initial unbiased MIRAS electron density map (cyan, contour level 1σ) with the final structure superimposed (blue coils, right side view). **b,** Anomalous difference Fourier map for selenomethionine-containing head module (magenta, contour level 2.5σ) with an outline of the structure superimposed (blue ribbon, right side view). Sulphur atoms of methionine residues are shown as green spheres. **c,** $F_o - F_c$ simulated annealing omit maps (cyan, contour level 3σ) with the final model superimposed, shown as sticks with carbon atoms coloured by subunit (see Fig. 2c). Shown are three regions of the head module, Med17 helix α3 (left), a part of the nose (middle), and a part of Med6 (right). Med17 residues 186 to 204, Med17 residues 515 to 533, and Med6 residues 78 to 92 were omitted in the map calculation, respectively. **d,** $F_o - F_c$ simulated annealing omit maps (cyan, contour level 3σ) for Med11 and Med22 linker regions (left and middle, respectively) and the Med17 β-sheet from the 'joint' (right). The final model is superimposed, shown as ribbons and coloured according to subunits (see Fig. 2c). Med17 helix α4 was omitted for clarity.

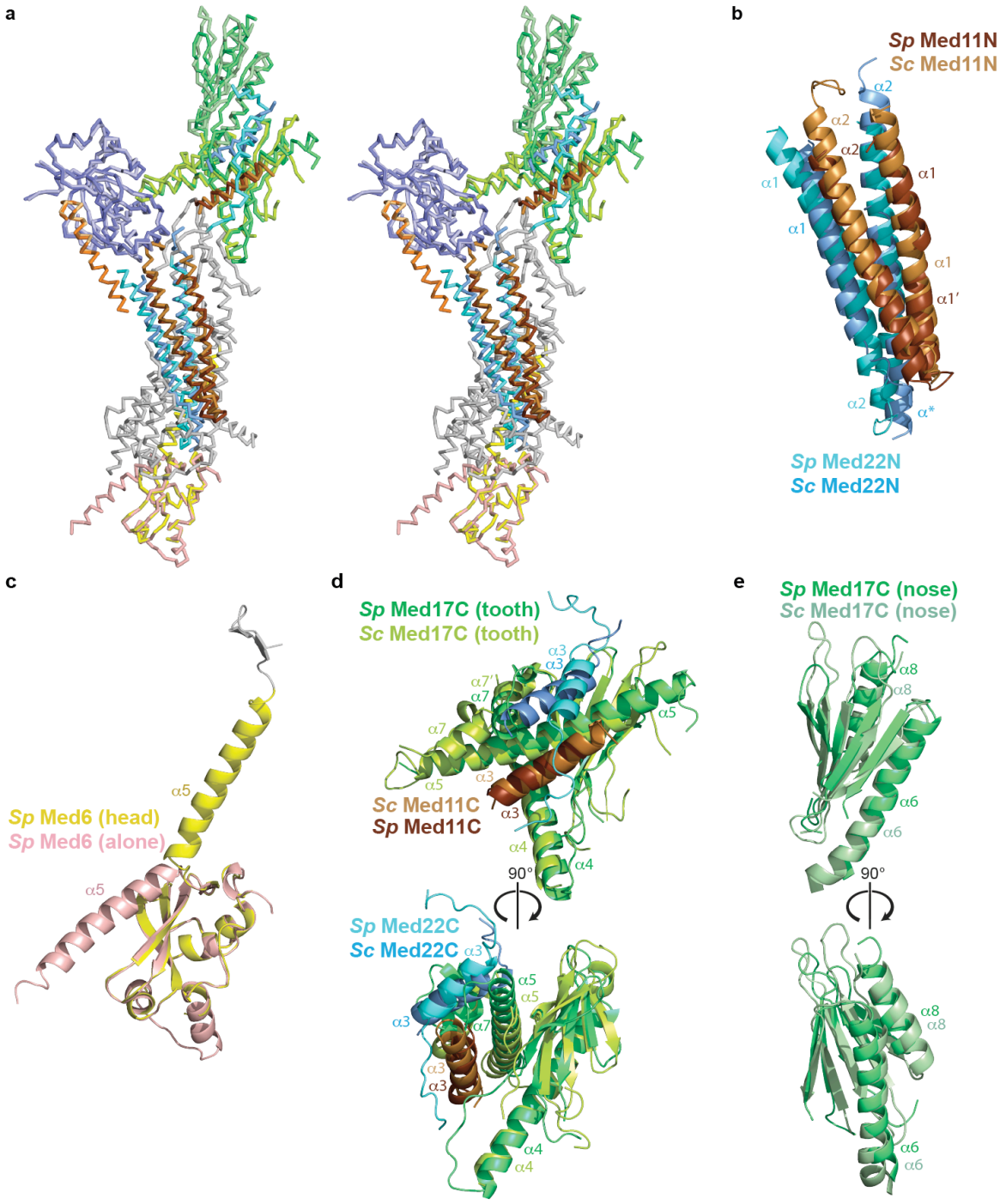

Supplementary Figure 5 | Higher resolution structures of Mediator head subunits and subcomplexes guided *Sp* head module modelling. a, Prior structures of Mediator head subunits or subcomplexes are superimposed on the final model of the *Sp* head module crystal structure, shown as α-carbon trace-in stereo view. *Sp* subunits are coloured as in Fig. 2c. *Sp* Med8C–Med18 (ref. 4), *Sc* Med11N–Med22N[7], *Sc* Med17C–Med11C–Med22C (this work) and isolated *Sp* Med6 (this work) are superimposed. Protein regions with no prior atomic structural information are shown in gray. For extra detail, **b,** *Sc* Med11N–Med22N **c,** *Sp* Med6, **d,** *Sc* Med17C–Med11C–Med22C 'tooth' and **e,** *Sc* Med17C 'nose' are superimposed on the corresponding regions of the *Sp* head module and shown in ribbon.

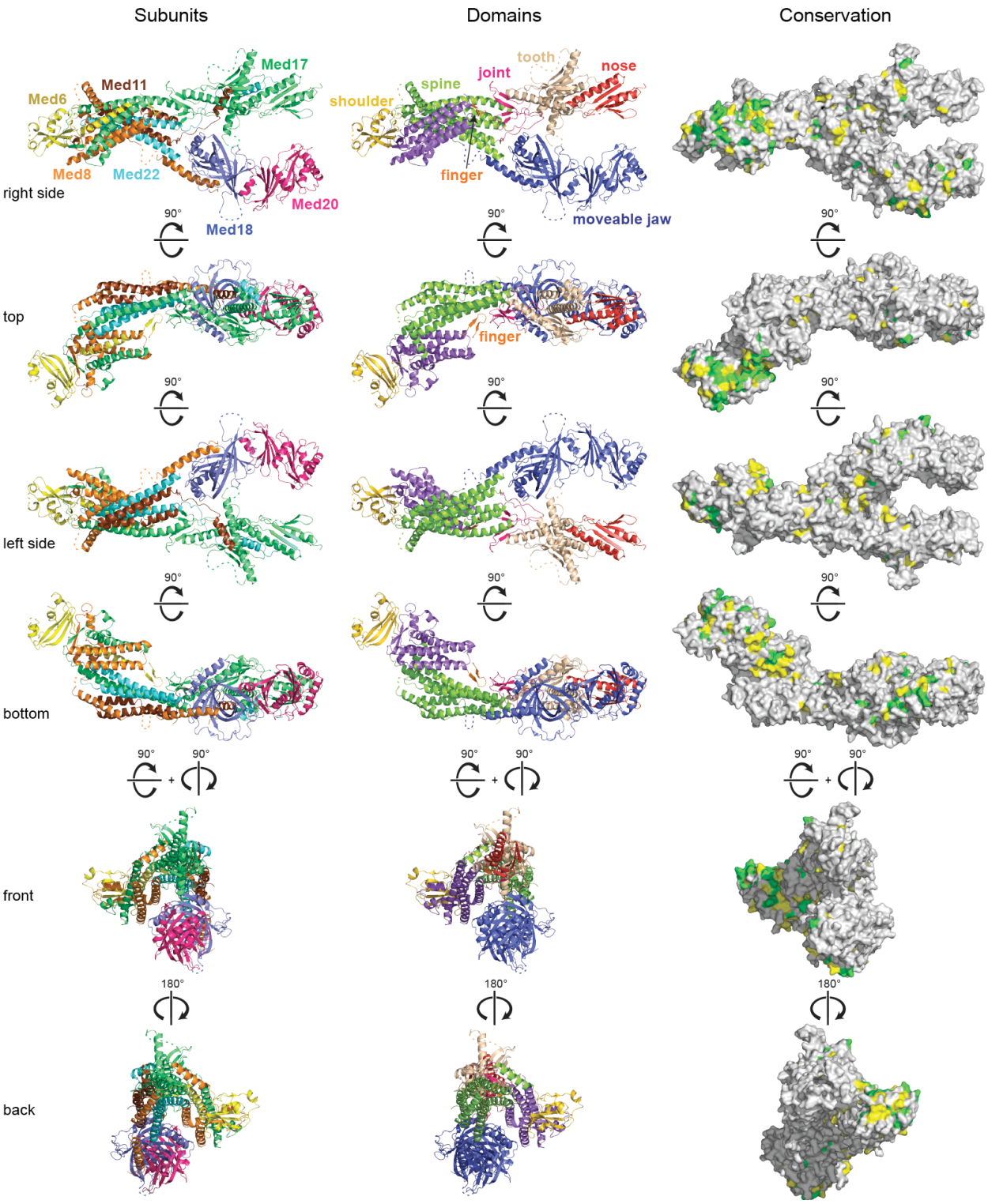

Supplementary Figure 6 | Structure, organization and surface conservation of *Sp* Mediator head module. The head module is represented as ribbon (left and middle), coloured by subunit (left) or according to structural elements (middle). Surface representation (right) reveals several conserved surface regions. Residues which are invariant or conserved among the seven yeast species *Sp*, *Sc*, *Candida glabrata*, *Candida albicans*, *Ashbya gossypii*, *Kluyveromyces lactis* and *Debaryomyces hansenii* are coloured in green or yellow, respectively (see Supplementary Fig. 1).

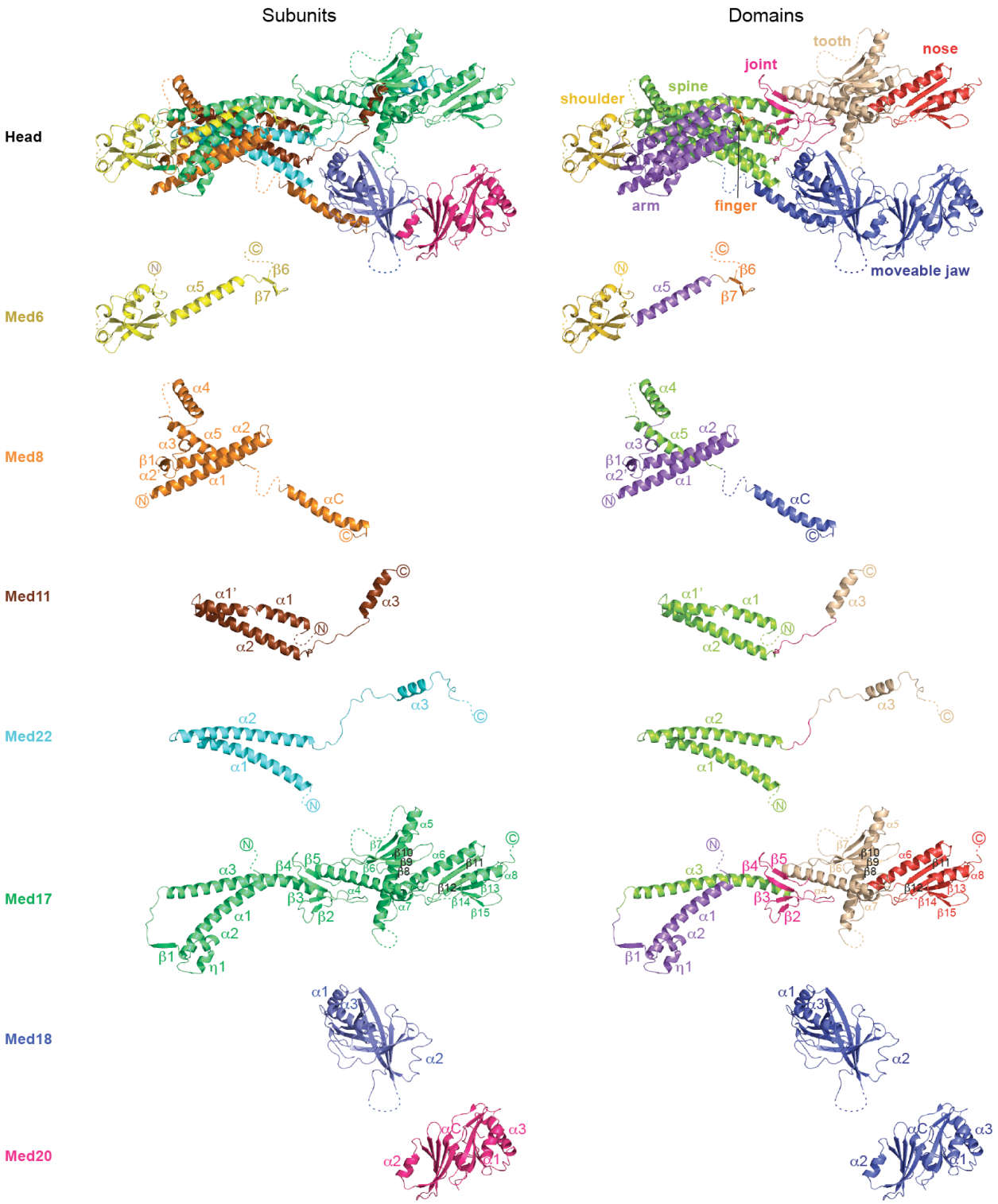

Supplementary Figure 7 | Subunit structure within the *Sp* Mediator head module. The head module and its individual subunits are represented as ribbons (right side view), coloured by subunit (left) or according to structural elements (right).

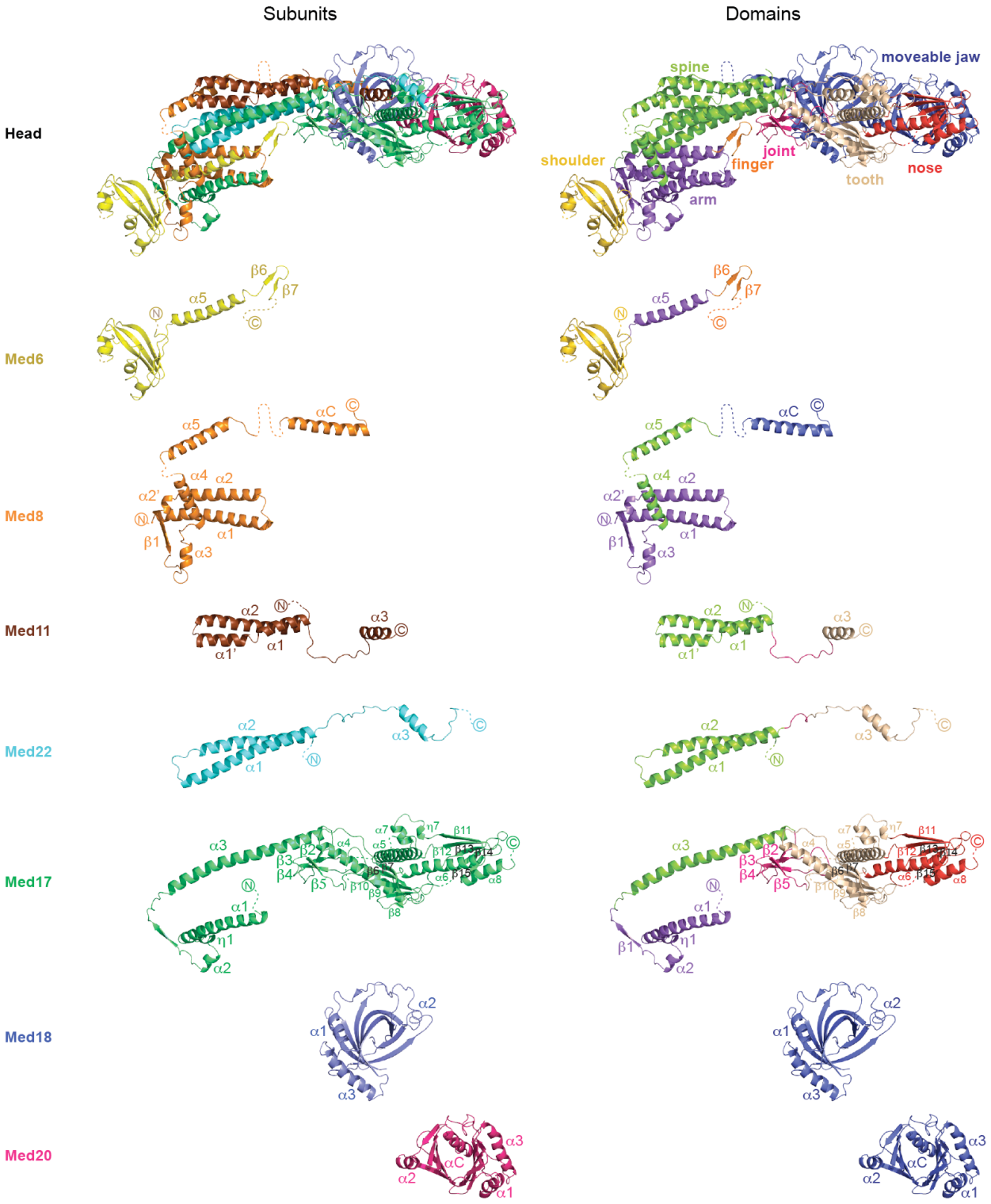

Supplementary Figure 8 | Subunit structure within the *Sp* Mediator head module. The head module and its individual subunits are represented as ribbons (top view), coloured by subunit (left) or according to structural elements (right).

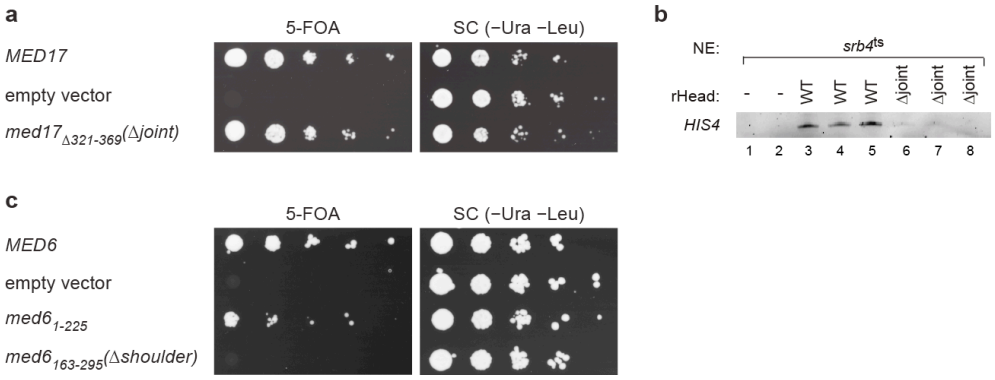

Supplementary Figure 9 | Structural element deletions affect Mediator head function *in vivo* and *in vitro*. **a,** Yeast complementation assays were performed with wild-type *MED17*, an empty vector, or *MED17* lacking the joint (Δjoint, Δ321-369) as described (see Methods). **b,** *In vitro* transcription was performed with extract from the *srb4-138* (*srb4*^{ts}) strain in the absence of recombinant head module (rHead; lanes 1-2), in the presence of 5 pmol wild-type rHead (lanes 3-5), or 5 pmol rHead Δjoint (lanes 6-8) as described (see Methods). **c,** Yeast complementation assays were performed with wild-type *MED6*, an empty vector, a *MED6* variant corresponding to the construct used for the *Sp* head module crystallization (residues 1-225), or *MED6* lacking the shoulder (Δshoulder, residues 163-295) as described (see Methods).

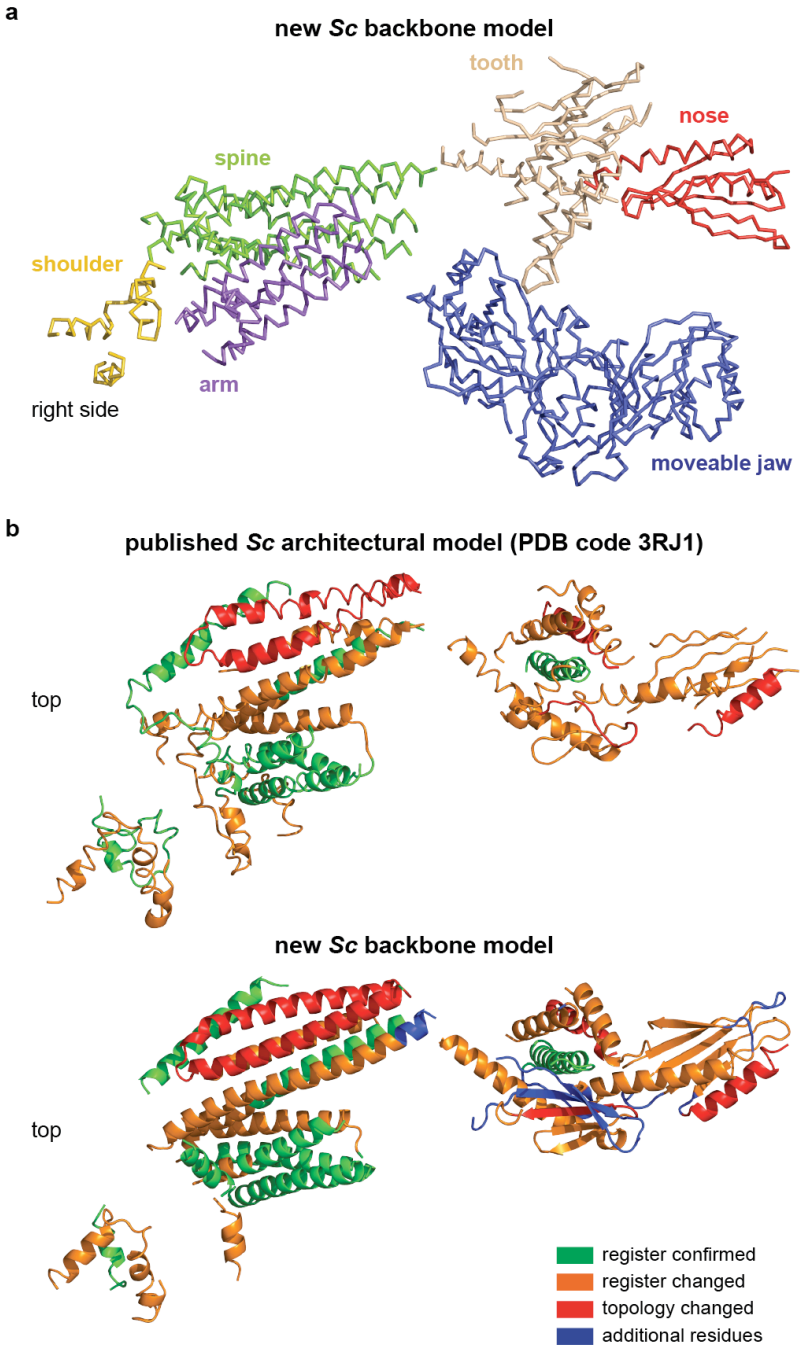

Supplementary Figure 10 | A new model for the *Sc* Mediator head module. a, Backbone homology model of the *Sc* head module based on a published electron density[15]. The model is shown as a Cα chain trace. The joint, finger and five protein linkers could not be modelled. The arm and shoulder could be modelled partially. **b,** Comparison of the published architectural model[15] of the *Sc* Mediator head module (top) with the new backbone model derived in this work (bottom). Both models are represented as ribbons. Secondary structure elements were defined automatically using DSSP[16]. The moveable jaw, which is similar in both models, was omitted for clarity. Regions for which the register was confirmed are in green, regions for which the register had to be changed are in orange. Elements for which the topology had to be corrected are in red. Regions that could be added are in blue.

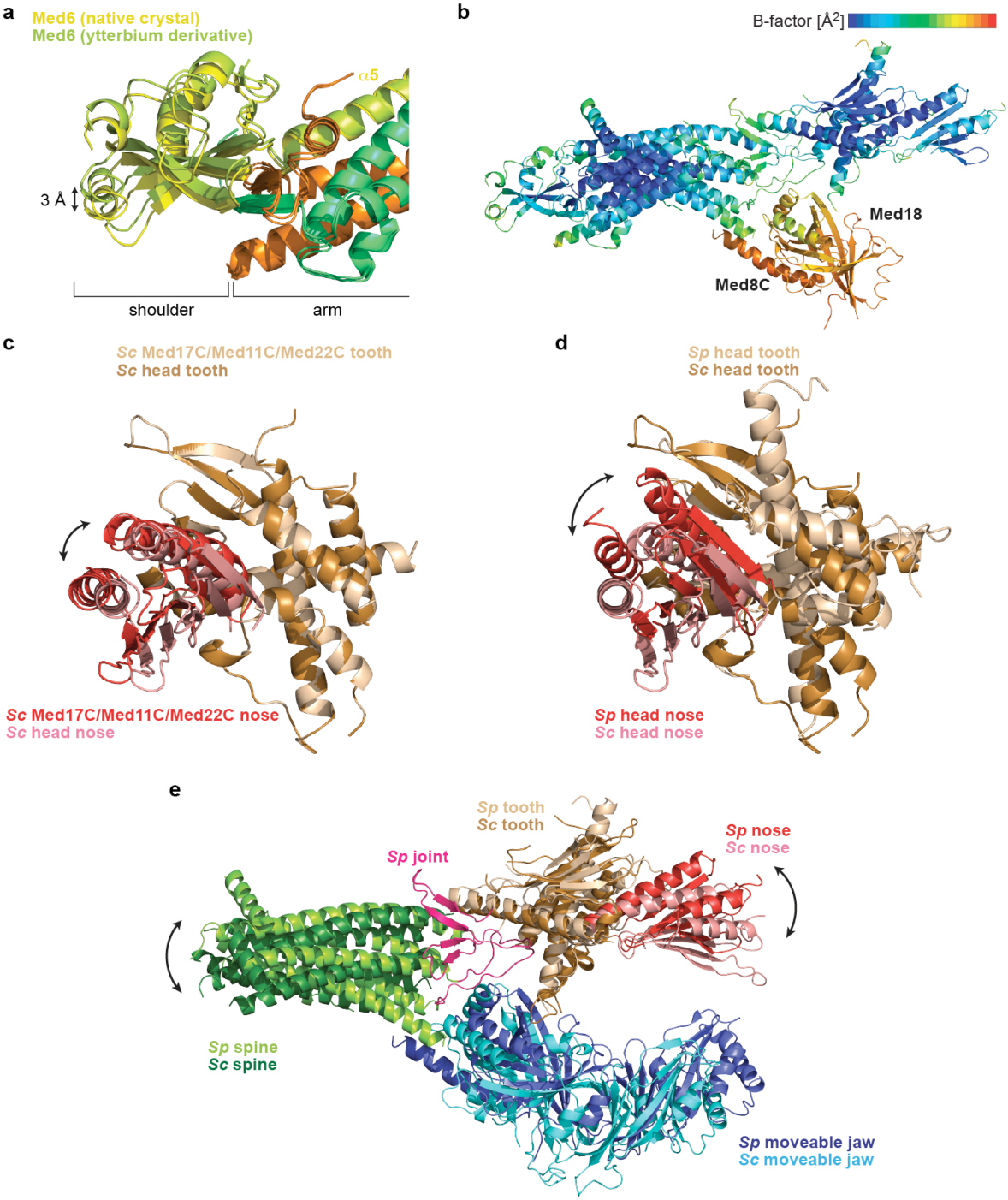

Supplementary Figure 11 | Structural comparisons reveal head module flexibility. a, The shoulder adopts different orientations relative to the arm in different Sp head module crystals. **b,** B-factor distribution within the refined *Sp* head module structure reveals a high degree of flexibility of the moveable jaw. **c,** Comparison of the orientation of the nose relative to the tooth between the new *Sc* head module backbone model and the free *Sc* Med17C–Med11C–Med22C structure. Tooth elements are superimposed. **d,** Comparison of the orientation of the nose relative to the tooth between the new *Sc* head module backbone model and the *Sp* head module structure. Tooth elements are superimposed. **e,** Superposition of *Sc* and *Sp* tooth elements reveals a different orientation of the spine relative to the jaws. Arm, shoulder and finger elements were omitted for clarity.

Table 3 | Mediator head module mutations, their location, and predicted effect

Yeast strain	Site(s) in *Sc* (*Sp*)	Location	Predicted effect	Ref.
med6-ts1	F31S (F37)	Med6, shoulder	Fold destabilization	5
med6-ts2	Q49L (Q55)	Med6, shoulder	Fold destabilization	5
	I68L (α3-α4)	Med6, shoulder	Unknown	
	L94P (α3-α4)	Med6, shoulder	Unknown	
	F125Y (L88)	Med6, shoulder	Intersubunit destabilization	
	R132G (N95)	Med6, shoulder	Fold destabilization	
	F194L (Y149)	Med6, finger	Intersubunit destabilization	
med6-ts6	L28P (L34)	Med6, shoulder	Fold destabilization	5
	K47T (K53)	Med6, shoulder	Fold destabilization	
	T134A (L97)	Med6, shoulder	Unknown	
	Q171R (A126)	Med6, shoulder	Intersubunit destabilization	
	T177M (A132)	Med6, arm	Intersubunit destabilization	
	M273L (β7-C-term)	Med6 (n/a)	Unknown	
	I275V (β7-C-term)	Med6 (n/a)	Unknown	
MED6-101	D152Y (V107)	Med6, shoulder	Intersubunit stabilization	6
med11-ts1	E17K (E28)	Med11, spine	Intersubunit destabilization	7
	L24K (L35)	Med11, spine	Intersubunit destabilization	
T31A*	T31A (I42)	Med11, spine	Intersubunit destabilization	8
L66P*	L66P (L72)	Med11, spine	Fold destabilization	8
G92S*	G92S (Y95)	Med11, joint	Intersubunit destabilization	8
srb4-138	L21S (L18)	Med17 (n/a)	Not required for *ts*	2,3
	N24I (E21)	Med17 (n/a)	Unknown	
	L124M (L56)	Med17 (n/a)	Not required for *ts*	
	S226P (S127)	Med17, arm	Fold destabilization	
	M313I (V209)	Med17, spine	Unknown	
	E460G (T329)	Med17, tooth	Fold destabilization	
	E583G (β11-α7)	Med17, nose	Unknown	
	F649S (D513)	Med17, nose	Fold destabilization	
SRB4-1	G353C (G242)	Med17, joint	Intersubunit stabilization	12
SRB4-101	E286K (S182)	Med17, spine	Intersubunit stabilization	5
med17-68	P370S (S257)	Med17, joint	Fold destabilization	10
	L441P (I310)	Med17, tooth	Fold destabilization	
med17-158	F159Y (N-term-α1)	Med17 (n/a)	Unknown	10
	S226T (S127)	Med17, arm	Fold destabilization	
	K280M (K176)	Med17, spine	Intersubunit destabilization	
	K377N (β5-β6)	Med17, joint	Unknown	
	E438G (E307)	Med17, tooth	Fold destabilization	
	V465E (I333)	Med17, tooth	Fold destabilization	
med17-208	N611H (N476)	Med17, nose	Unknown	10
	A655T (β14-β15)	Med17, nose	Unknown	
	E669D (E525)	Med17, nose	Unknown	
med17-257	L520S (D405)	Med17, tooth	Intersubunit destabilization	10
	I541K (I424)	Med17, nose	Fold destabilization	
	E669G (E525)	Med17, nose	Unknown	
med17-327	M442V (W311)	Med17, tooth	Fold destabilization	10
	V670E (V526)	Med17, nose	Fold destabilization	
med17-sup1	I128V (L60)	Med17 (n/a)	Unknown	10

	R582G (β11-α7)	Med17, nose	Unknown	
	N595D (P459)	Med17, tooth	Unknown	
SRB5-1	T22I (S21)	Med18, movable jaw	Intersubunit stabilization	12
SRB2-1	P14H (A15)	Med20, movable jaw	Unknown	13
SRB6-1	N86K (N84)	Med22, spine	Intersubunit stabilization	12
med22-ts1	L73E (L71)	Med22, spine	Intersubunit destabilization	7
	K80E (K78)	Med22, spine	Intersubunit destabilization	
SRB6-201	N59H (E57)	Med22, spine	Intersubunit stabilization	6
Human	**Site in *Hs* (*Sc*, *Sp*)**	**Location**	**Predicted effect**	**Ref.**
Hs L371P	L371P (M504, L389)	Med17, tooth	Fold destabilization	11

Sc, Saccharomyces cerevisiae; *Sp*, Schizosaccharomyces pombe; *Hs*, Homo sapiens; Ref., Reference. Residues with no equivalent in *Sp* were annotated by the N- and C-terminal secondary structure elements closest to that residue ('secondary structure'-'secondary structure'). When mutations fell within three amino acids of the built *Sc* or *Sp* models, they were included in Figs 4b or 4c, respectively for illustrative purposes.

* Med11 mutations were numbered according to the corrected annotation[7]. T31A, L66P and G92S refer to T47A, L82P and G108S, respectively in the original publication[8].

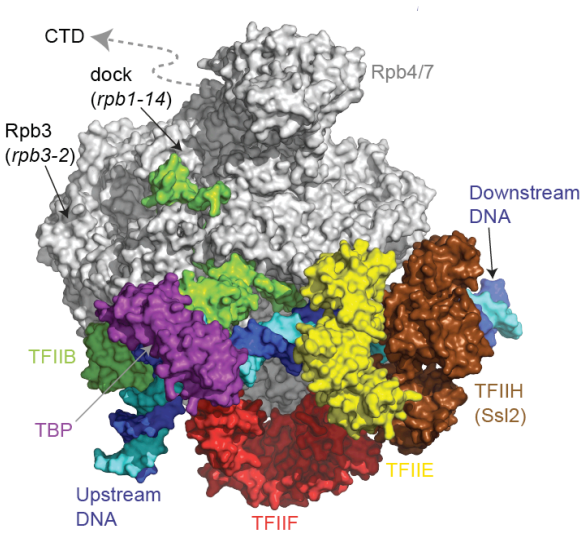

Supplementary Figure 12 | Surface representation of the current Pol II transcription pre-initiation model[17] and head module interaction. Pol II is in silver, DNA in blue and cyan, and general transcription factors are in different colours. The view reveals the putative head module interaction face around subunit Rpb3, the dock domain, the CTD, and the Rpb4/7 subcomplex.

Supplementary References

1 Seizl, M. *et al.* A conserved GA element in TATA-less RNA polymerase II promoters. *PloS one* 6, e27595, doi:10.1371/journal.pone.0027595 (2011).

2 Thompson, C. M. & Young, R. A. General requirement for RNA polymerase II holoenzymes in vivo. *Proceedings of the National Academy of Sciences of the United States of America* 92, 4587-4590 (1995).

3 Takagi, Y. & Kornberg, R. D. Mediator as a general transcription factor. *The Journal of biological chemistry* 281, 80-89, doi:10.1074/jbc.M508253200 (2006).

4 Lariviere, L. *et al.* Structure-system correlation identifies a gene regulatory Mediator submodule. *Genes & development* 22, 872-877, doi:10.1101/gad.465108 (2008).

5 Lee, Y. C. & Kim, Y. J. Requirement for a functional interaction between mediator components Med6 and Srb4 in RNA polymerase II transcription. *Molecular and cellular biology* 18, 5364-5370 (1998).

6 Lee, T. I. *et al.* Interplay of positive and negative regulators in transcription initiation by RNA polymerase II holoenzyme. *Molecular and cellular biology* 18, 4455-4462 (1998).

7 Seizl, M., Lariviere, L., Pfaffeneder, T., Wenzeck, L. & Cramer, P. Mediator head subcomplex Med11/22 contains a common helix bundle building block with a specific function in transcription initiation complex stabilization. *Nucleic acids research* 39, 6291-6304, doi:10.1093/nar/gkr229 (2011).

8 Esnault, C. *et al.* Mediator-dependent recruitment of TFIIH modules in preinitiation complex. *Molecular cell* 31, 337-346, doi:10.1016/j.molcel.2008.06.021 (2008).

9 Takagi, Y. *et al.* Head module control of mediator interactions. *Molecular cell* 23, 355-364, doi:10.1016/j.molcel.2006.06.007 (2006).

10 Soutourina, J., Wydau, S., Ambroise, Y., Boschiero, C. & Werner, M. Direct interaction of RNA polymerase II and mediator required for transcription in vivo. *Science* 331, 1451-1454, doi:10.1126/science.1200188 (2011).

11 Kaufmann, R. *et al.* Infantile cerebral and cerebellar atrophy is associated with a mutation in the MED17 subunit of the transcription preinitiation mediator complex. *American journal of human genetics* 87, 667-737, doi:10.1016/j.ajhg.2010.09.016 (2010).

12 Thompson, C. M., Koleske, A. J., Chao, D. M. & Young, R. A. A multisubunit complex associated with the RNA polymerase II CTD and TATA-binding protein in yeast. *Cell* 73, 1361-1375 (1993).

13 Nonet, M. L. & Young, R. A. Intragenic and extragenic suppressors of mutations in the heptapeptide repeat domain of Saccharomyces cerevisiae RNA polymerase II. *Genetics* 123, 715-724 (1989).

14 Karplus, P. A. & Diederichs, K. Linking crystallographic model and data quality. *Science* 336, 1030-1033, doi:10.1126/science.1218231 (2012).

15 Imasaki, T. *et al.* Architecture of the Mediator head module. *Nature* 475, 240-243, doi:10.1038/nature10162 (2011).

16 Kabsch, W. & Sander, C. Dictionary of protein secondary structure: pattern recognition of hydrogen-bonded and geometrical features. *Biopolymers* 22, 2577-2637, doi:10.1002/bip.360221211 (1983).

17 Grunberg, S., Warfield, L. & Hahn, S. Architecture of the RNA polymerase II preinitiation complex and mechanism of ATP-dependent promoter opening. *Nature structural & molecular biology*, doi:10.1038/nsmb.2334 (2012).